Induced Fe and Mn magnetic moments in Co-FeMn bilayers on Cu(001)

F. Offi,* W. Kuch,† L. I. Chelaru, K. Fukumoto, M. Kotsugi, and J. Kirschner
Max-Planck-Institut für Mikrostrukturphysik, Weinberg 2, D-06120 Halle, Germany
(Received 29 July 2002; revised manuscript received 18 November 2002; published 25 March 2003)

Using photoemission electron microscopy in combination with x-ray magnetic circular dichroism, element selective magnetic domain images have been obtained from single-crystalline Co/FeMn and FeMn/Co bilayers epitaxially grown on a Cu(001) single crystal. The contact with ferromagnetic Co leads to the observation of a net magnetic moment in Fe and Mn, independently of the paramagnetic or antiferromagnetic state of the FeMn thin films. Only a small fraction of this moment might mediate the magnetic interaction at the interface, and thus be responsible for the exchange bias effect.

DOI: 10.1103/PhysRevB.67.094419 PACS number(s): 75.50.Ee, 75.60.Ch, 75.70.Cn

I. INTRODUCTION

The phenomena resulting from the interaction between a ferromagnetic (FM) and an antiferromagnetic (AFM) material have received an increasing interest both from an experimental[1] and a theoretical[2] point of view over the last decade. The flourishing of studies is also connected to applications of FM-AFM systems in spin-valve devices,[3] exploiting the fact that the hysteresis loop of these systems is displaced along the applied field axis by an amount referred to as *exchange bias* field. Notwithstanding the large number of investigations, a complete understanding of the magnetic coupling at FM-AFM interfaces still is unavailable. In particular, a frequently addressed issue is the role of uncompensated AFM spins. Here the term ''uncompensated'' refers to spins within the interface atomic layer of the AFM which are not compensated by spins of another direction within the same layer, and thus lead to a net magnetic moment of that layer. For example, the original model proposed by Meiklejohn and Bean[4] and the more recent calculations of Schulthess and Butler[5] lead to a nonshifted hysteresis loop when the AFM interface is compensated, i.e., if there is no net magnetic moment in that layer. Net magnetic moments at the interface of an AFM material were first observed in CoO, induced by a field cooling procedure.[6] The observation of net moments at the interface has also been claimed in $Fe_{50}Mn_{50}$ sputtered film, sandwiched between Co and $Ni_{81}Fe_{19}$,[7] where about half of the observed moments switched with the ferromagnetic layer, and the other half did not. A net Ni moment has been observed in NiO/Co bilayers,[8] but its exact origin was not specified. Finally a net Ni moment, induced in NiO by deposition of FM Co, has been investigated by x-ray absorption microspectroscopy, and correlated to the coercivity increase in exchange biased systems.[9]

In order to investigate the possible presence of uncompensated AFM spins in FM-AFM systems and their influence on the magnetic coupling at the interface, we used epitaxial Co/FeMn and FeMn/Co bilayers on a Cu(001) single crystal. Epitaxial bilayers present some advantages compared with polycrystalline films obtained by sputtering techniques: They have smoother interfaces, and no grains of different crystal orientation are present, which may influence the magnetic interaction. By using metallic bilayers, oxidation-reduction reactions complicating the situation at oxide-metal interfaces are also absent.

Magnetic domain images have been taken from the Co/FeMn bilayers by using a photoelectron emission microscope (PEEM). X-ray magnetic circular dichroism (XMCD) has been used as magnetic contrast mechanism, where the excitation was supplied by circularly polarized x rays from a synchrotron radiation source. One of the capabilities of the technique, which turned out to be particularly useful for the present experiments, is its element selectivity, and the possibility to access buried layers. It has been therefore possible to image the domain configuration for both the Co/FeMn and the FeMn/Co bilayers on Cu(001), at the same time for all three magnetic elements. Due to the depth sensitivity of the electron yield detection method that is used by PEEM, the signal from each atomic layer is differently attenuated. This leads to an exponentially weighted averaging with an exponential decay length of about 2 nm.[10] A small net magnetic moment would thus be also observed by XMCD from an uncompensated AFM, in which a net moment in the surface or interface plane is accompanied by an opposite moment in the adjacent plane. While no net magnetic moment is found in FeMn films on Cu(001), we do observe a net magnetic moment for both elements, Fe and Mn, induced by the contact with an FM Co film. When FeMn is in the AFM state, a small part of this induced moment can be interpreted as uncompensated AFM spins which mediate the magnetic interaction at the interface.

As a matter of fact direct imaging of AFM domains by using PEEM in combination with x-ray magnetic linear dichroism, successfully applied to $LaFeO_3$ (Ref. 11) and NiO,[12,13] gave no result for the present studied AFM FeMn. A reason for this can be found in the crystal field splitting of the absorption peaks, which is present in $LaFeO_3$ and NiO oxides, but nearly vanishes in the metallic FeMn films, thus greatly reducing the linear dichroism. Another reason could be possibly a noncollinear spin structure of the FeMn thin films.

II. EXPERIMENT

The experiments were performed in an ultrahigh vacuum chamber with a base pressure of 10^{-8} Pa. The Cu substrate was a disk-shaped single crystal with the [001] direction nor-

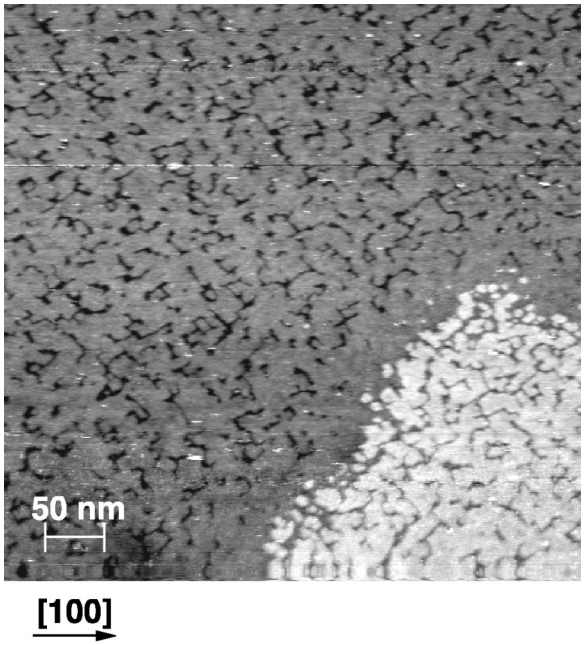

FIG. 1. Scanning tunneling microscopy image of a 12.9 ML $Fe_{50}Mn_{50}$ film on Cu(001). The field of view is 500×500 nm^2. The crystallographic orientation is indicated at the bottom of the figure. Large atomically flat terraces with many small holes, one atomic layer deep, are observed.

mal to the surface. The films were grown on the clean substrate at room temperature in zero field by electron beam assisted thermal evaporation. Fe and Co were evaporated from high purity wires (99.99% purity) of 2 mm diameter, while for Mn a rod (99.5% purity) of 4 mm diameter was used. FeMn alloys were obtained by simultaneous evaporation of Fe and Mn from two different sources. During deposition the pressure in the chamber could be kept below 5×10^{-8} Pa. Composition and film thickness were calibrated by means of oscillations in the medium energy electron diffraction intensity recorded during evaporation, and cross checked by Auger electron spectroscopy. More details about the structural and magnetic properties of the Co/FeMn bilayers on Cu(001) are given elsewhere.[14] The bilayers were grown as crossed double wedges, as described in a previous publication,[15] resulting in 150 μm wide wedges and a 350 μm wide plateau of uniform film thickness at the upper end of the wedge.

Figure 1 shows the scanning tunneling microscopy (STM) image of a 500×500 nm^2 area of a 12.9 ML $Fe_{50}Mn_{50}$ on Cu(001). Large flat terraces of the size of substrate terraces are observed. The area in the lower right of the image belongs to the next terrace, one monoatomic step higher. The terraces are dotted with small elongated holes of one atomic layer depth, on average being about 30 nm long and 5 nm wide. Although it cannot be directly concluded that the FeMn surface morphology after deposition of a Co film on top of it stays exactly the same as that imaged by STM, it is still clear that the films grow in a very defined way with an extremely low interface roughness.

Magnetic domain images were obtained at room temperature from the asymmetry of the local secondary electron intensity at the elemental L_3 absorption edge upon helicity reversal of circularly polarized excitation. The magnetic contrast is thereby provided by x-ray magnetic circular dichroism,[16] that is the difference in x-ray absorption cross section upon helicity reversal. The secondary electrons, the intensity of which is proportional to the absorption, are then spatially imaged by the PEEM. The experiments were performed at the UE56-2/PGM2 beamline of the Berlin synchrotron radiation facility BESSY II. The light was incident under an angle of 30° to the sample surface, with an azimuth angle of 7° from the [110] axis of the Cu substrate. The setup of the photoemission microscope is identical to that described in previous publications.[17–19] Parameters were set to result in a lateral resolution of 400 nm and a field of view of 90 μm.

III. RESULTS

Bulk $Fe_{50}Mn_{50}$ alloy is an antiferromagnet with a Néel temperature of about 500 K.[20] No magnetic domain images could be detected by XMCD-PEEM for any of the $Fe_{50}Mn_{50}$ films deposited on Cu(001), even after heating and cooling in an external magnetic field. The situation is different when the alloy film is in contact with a ferromagnetic Co film, that is when the Co thickness is bigger than 2 atomic monolayers (ML) at room temperature. In this case an XMCD signal from Fe and Mn was detected, resulting in the images shown in Fig. 2. The three images show the domain patterns of Co, Fe, and Mn of the same area of a Co/$Fe_{50}Mn_{50}$/Cu(001) sample. The Co and $Fe_{50}Mn_{50}$ films were grown as crossed double wedges, as schematically displayed in the sketch in the lower right part of the figure. The $Fe_{50}Mn_{50}$ thickness (t_{FeMn}), indicated at the left axes of the images, increases from bottom to top. The Co thickness (t_{Co}), increasing from left to right, is indicated for all three images at the bottom axis of the Mn image. The direction of the crystallographic axes is shown at the right of the images in the rectangular box. The big arrow at 52° from the [100] direction displays the direction of the incoming x rays ($h\nu$). In the Co image, one can see the characteristic behavior for Co growing on top of $Fe_{50}Mn_{50}$. For $t_{FeMn}<10$ ML relatively big domains can be seen, oriented along two of the four $\langle110\rangle$ azimuth directions, as indicated by the arrows inside some domains. The domains are much smaller for $t_{FeMn}>10$ ML: as discussed in Ref. 21, this is due to the antiferromagnetic state of $Fe_{50}Mn_{50}$ for thicknesses bigger than 10 ML. In the Fe and Mn images the same domain pattern as in the Co image can be recognized, however with a lower contrast. The typical maximum contrast in Fe and Mn is approximately just 5% of the contrast in Co. The total time for acquisition of the Co and Fe images was around 10 min each, while it was twice that time for Mn. The resulting different noise level is the reason why the Mn image appears sharper than the Fe one.

A small XMCD signal has also been obtained from Fe and Mn for the reversed order of deposition, when the $Fe_{50}Mn_{50}$ film is deposited on top of Co/Cu(001). This is shown in Fig. 3, where a $Fe_{50}Mn_{50}$/Co/Cu(001) sample is imaged by tuning the x-ray photon energy to the Co, Fe, and Mn L_3 absorption edges. At the bottom of the figure a sketch of the

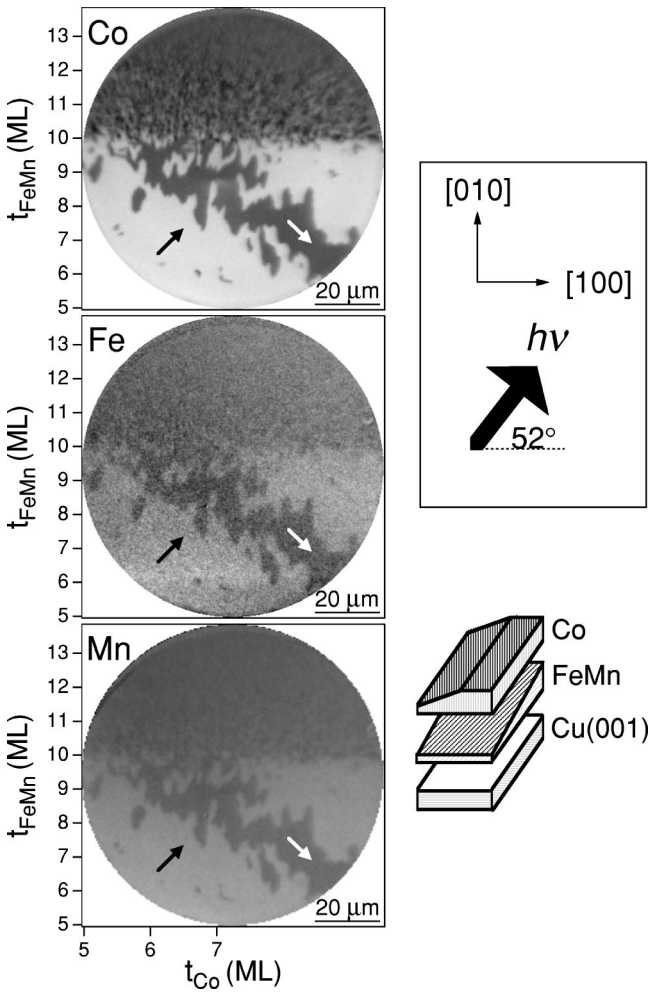

FIG. 2. Co, Fe, and Mn domain patterns of the same area of a $Co/Fe_{50}Mn_{50}/Cu(001)$ sample. $Fe_{50}Mn_{50}$ and Co thicknesses (t_{FeMn} and t_{Co}) are indicated at the left and bottom axes of the images, respectively. The box at the right of the images contains the direction of the incoming x rays ($h\nu$) and the crystallographic axes. A schematic sketch shows the sample.

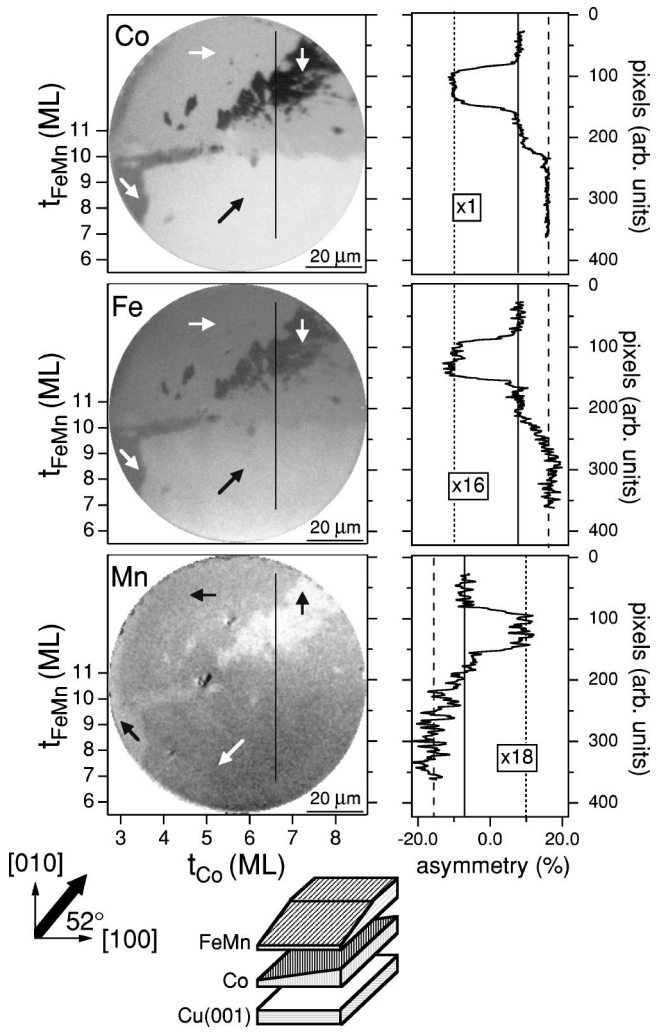

FIG. 3. Left column, Co, Fe, and Mn domain patterns of the same area of a $Fe_{50}Mn_{50}/Co/Cu(001)$ sample. Thicknesses are indicated at the images axes. Right column, Result of line scans along the black lines printed in each image in the left column. At the bottom of the figure a sketch of the sample is given. Direction of the incoming x rays ($h\nu$) and crystallographic axes are indicated.

sample is given, and the crystallographic axes and the incoming x rays' direction ($h\nu$) are indicated. The $Fe_{50}Mn_{50}$ thickness is shown at the left axes of the images, increasing from bottom to top, and the Co thickness at the bottom axis of the Mn image, increasing from left to right. A change in the Co domain pattern can be seen at the $Fe_{50}Mn_{50}$ transition from paramagnetic (PM) to antiferromagnetic. For $t_{FeMn} > 10$ ML the magnetization direction, indicated by the arrows in the domains, is rotated from the $\langle 110 \rangle$ crystallographic axes to the $\langle 100 \rangle$ crystallographic axes. A small XMCD asymmetry is detectable again also for Fe, as displayed by the domain pattern of the Fe image. From this domain pattern one concludes that the Fe induced net magnetic moment is coupled ferromagnetically to the Co moment. Interestingly the contrast is reversed in the Mn image. For example, the black domain in Co, oriented along the $[0\bar{1}0]$ direction, becomes bright in the Mn image. The most likely conclusion is therefore that Mn has a small net moment, which is aligned antiferromagnetically to the Co magnetization and to the net Fe moment. In order to prove these considerations, an asymmetry scan along a line indicated in each image has been taken. The asymmetry values of the line scans are displayed in Fig. 3 on the right-hand side of the corresponding image. The scale of the vertical position in image pixels at the right axis of each line scan graph is the same as for the corresponding domain image. The asymmetry scale is indicated at the bottom axis of the Mn scan. In the Co scan one can see three levels of asymmetry, marked by the three vertical lines. These correspond to the three domains crossed by the black line printed in the Co image. The scans in the Fe and Mn images have been multiplied by the reported factors in order to be in the same scale as the Co one. One sees that the three asymmetry levels in the Fe and Mn scans are spaced exactly as in the Co scan. Therefore, the relative contrast in the domains is identical in Co, Fe, and Mn. This demonstrates that the observed Fe net moment is coupled ferromagnetically to Co, having the same magneti-

zation orientation in the different domains, while the observed Mn net moment is coupled antiferromagnetically to Co and Fe. Moreover, one can realize from the Fe and Mn images of Fig. 3 that an XMCD signal is detectable for both $t_{FeMn}<10$ ML and $t_{FeMn}>10$ ML. It means that whatever the magnetic state of the $Fe_{50}Mn_{50}$ alloy, PM or AFM, when in contact with a Co film it acquires an induced net ferromagnetic moment. This was not so clear from the images of Fig. 2, where the small domains in Fe and Mn for $t_{FeMn}>10$ ML are not fully resolved, possibly leading to the conclusion that no net magnetic moment is induced in Fe and Mn when the $Fe_{50}Mn_{50}$ film is in an AFM state. This is proven to be not true by the images in Fig. 3, obtained by reversing the deposition sequence.

Since images of magnetic domains in Fe and Mn could just be detected when $Fe_{50}Mn_{50}$ was in contact with an FM Co film, one possibility is that the observed net magnetic moment is induced in Fe and Mn mainly at the interface, i.e., close to the Co film. This cannot be tested definitively, since the way the magnetic images are obtained gives a weighted average along the direction perpendicular to the surface. A decreasing contrast in the Fe and Mn domain images with increasing $Fe_{50}Mn_{50}$ thickness, however, would be consistent with such an interpretation. It can be seen, for example, in the Fe case, in Fig. 4. The Co and Fe domain patterns from an $Fe_{50}Mn_{50}$/Co double-wedge bilayer on Cu(001) are shown in Figs. 4(a) and 4(b), respectively. The Co and Fe domain structures for a similar $Fe_{50}Mn_{50}$/Co sample with higher $Fe_{50}Mn_{50}$ thickness are displayed in Figs. 4(c) and 4(d), respectively. A sketch of the sample is given at the bottom of the figure. The $Fe_{50}Mn_{50}$ and Co thicknesses of the imaged sample area are indicated at the left axes, increasing from bottom to top, and at the bottom axis, increasing from left to right, respectively. The arrows in some domains indicate the magnetization direction. In the box at the bottom of the figure the crystallographic axes are indicated, along with the incoming x rays' direction ($h\nu$) at 52° from the [100] axis. By comparing Figs. 4(a) and 4(b) one can see that the Fe domain pattern is identical to the Co one. However, the domain in which the magnetization is oriented along the [110] direction in the Fe image is much brighter for an FeMn thickness between 0 and 3 ML than for higher thicknesses. In Fig. 4(d), the Fe domain pattern is shown for an FeMn thickness between 8 and 15 ML. Again the Fe domain structure is identical to the corresponding Co one, displayed in Fig. 4(c), but the Fe asymmetry does not display a strong dependence as a function of the FeMn thickness. This indicates that the asymmetry in Fe, proportional to the depth averaged net magnetic moment, is higher for the thinnest FeMn layers which are in direct contact with the Co film. In order to obtain more quantitative information, linescans of the asymmetry value along the $Fe_{50}Mn_{50}$ slope are extracted from the regions enclosed by the rectangles printed in the Co (a) and Fe (b) images, horizontally averaging over the width of the rectangles. The result of the linescans is reported in Fig. 6 and will be discussed in the following section.

Besides the induced net magnetic moments, another effect present in some of the Mn images is shown in Fig. 5. The Fe and Mn domain images printed in this figure were acquired

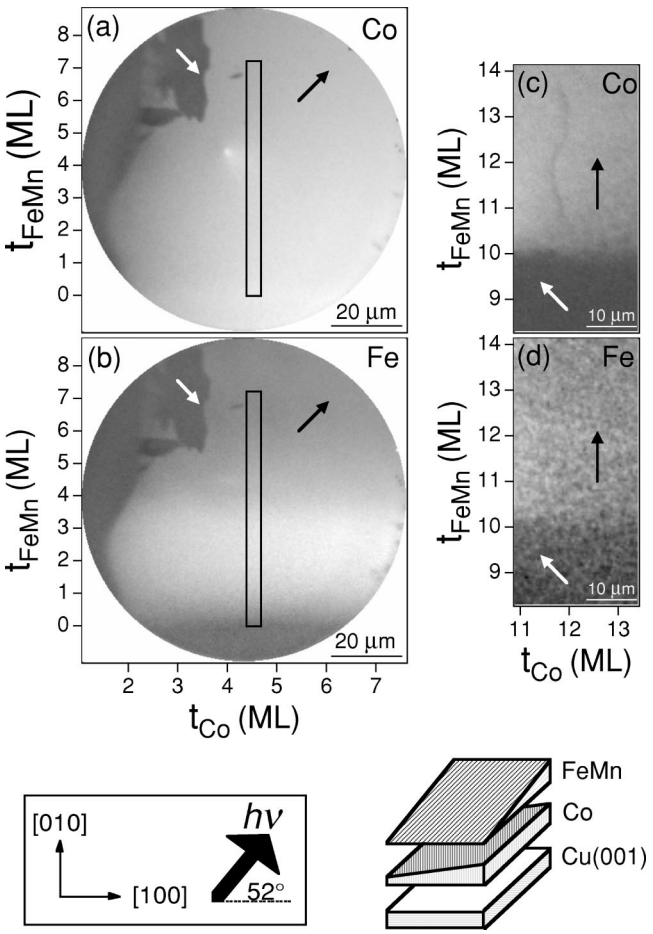

FIG. 4. Co (a) and Fe (b) domain patterns from the same area of an $Fe_{50}Mn_{50}$/Co double wedge on Cu(001). The domain structures in Co and Fe from a similar $Fe_{50}Mn_{50}$/Co sample for higher $Fe_{50}Mn_{50}$ thickness are displayed in (c) and (d), respectively. The sketch below the images shows the double-wedge structure of the sample. $Fe_{50}Mn_{50}$ and Co thicknesses are indicated at the left and bottom axes of the images, respectively. Crystallographic axes and direction of incoming x rays ($h\nu$) are indicated in the box below the images.

from the same area of an $Fe_{30}Mn_{70}$/Co/Cu(001) sample. The thicknesses of the two layers, grown as crossed double wedges (see sketch given in the figure), are indicated at the left axis for the $Fe_{30}Mn_{70}$ layer, increasing from bottom to top, and at the bottom axis for the Co layer, increasing from left to right. The Co domain pattern (not shown) is the same as the Fe domain pattern, just with a higher contrast. The Mn image displays the same domain pattern as the Fe image, but with a reversed contrast: The net moment of Mn is coupled antiparallel to Co and Fe, as in Fig. 3. Actually the magnetic domain pattern in Mn is almost hidden by stripes of alternating gray scale. One can notice that the stripes are perpendicular to the gradient of total thickness, i.e., to the sum of the increasing Co and $Fe_{30}Mn_{70}$ films thicknesses. Indeed in the region of constant Co thickness, for $t_{Co}>10$ ML, the contrast oscillates with the same 1 ML period of the $Fe_{30}Mn_{70}$ film thickness. On the other hand in the $Fe_{30}Mn_{70}$ plateau thickness region, for $t_{FeMn}>11$ ML, the alternating

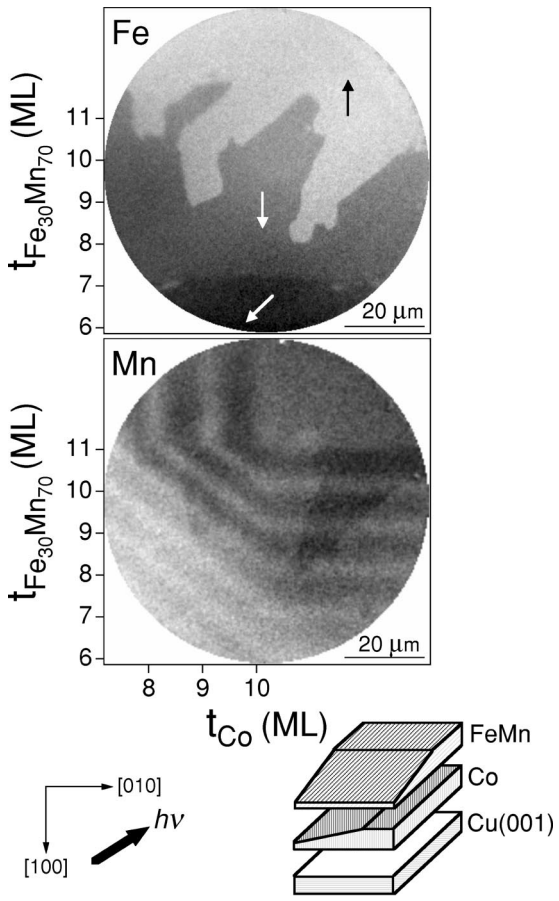

FIG. 5. Fe and Mn domain patterns of the same area of an $Fe_{30}Mn_{70}/Co/Cu(001)$ sample (see sketch). $Fe_{30}Mn_{70}$ and Co thicknesses are indicated at the left and bottom axes, respectively. Crystallographic axes, and incoming x-rays ($h\nu$) directions are displayed below the images. Regular stripes of different gray scale contrast can be seen in the Mn image, perpendicular to the gradient of total film thickness.

stripes correspond to the 1 ML period of the Co thickness. Finally in the area where both films are increasing in thickness, the stripes are perpendicular to the gradient of the sum of the thicknesses. It is worth to mention that the observation of these stripes is quite sensitive to the sample preparation conditions. In general, the intensity of the stripes has been found to be higher when the alloy wedge film is deposited on top of Co, especially when the Mn concentration is higher than 50% in the Fe_xMn_{100-x} film.

IV. DISCUSSION

As qualitatively shown in Fig. 4(b), the asymmetry in the Fe domain images is enhanced for very low $Fe_{50}Mn_{50}$ thickness. In order to obtain more quantitative information, a linescan of the asymmetry value along the $Fe_{50}Mn_{50}$ slope is extracted from the domain with magnetization along the [110] direction in Fig. 4(b), horizontally averaging over the black rectangle printed in the image. The linescan is shown by the solid line of Fig. 6, where the value of asymmetry is indicated at the left axis, and the $Fe_{50}Mn_{50}$ thickness at the

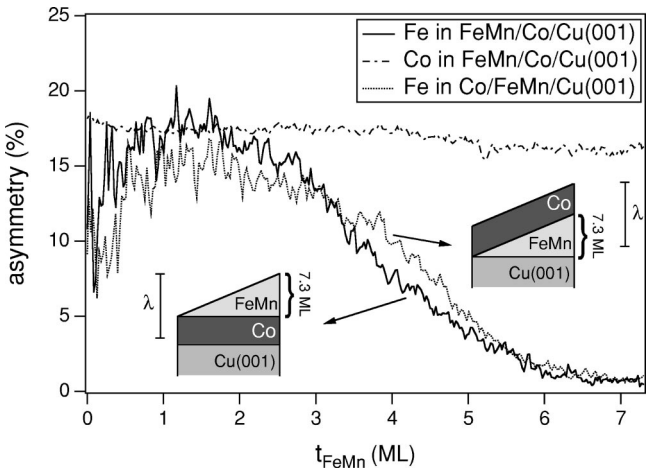

FIG. 6. Asymmetry in Fe and Co, taken from the domain images, as a function of FeMn thickness. The solid and dash dotted lines have been obtained by a line scan along the vertical axis of the rectangles printed in Figs. 4(b) and (a), respectively, horizontally averaging over the width of the rectangles. The dotted line displays the variation of asymmetry in a single domain in an Fe image from a $Co/Fe_{50}Mn_{50}/Cu(001)$ sample. Sketches of the sample's structures are given. The vertical bars labeled as λ indicate the effective electron escape depth and are to scale with the sample thickness of the sketches.

bottom axis, spanning from 0 to 7.3 ML. A sketch shows the structure of the sample. The vertical bar labeled with λ indicates the effective escape depth of the secondary electrons (see below) and is drawn to scale with the sample thickness of the sketch. The asymmetry displays indeed a strong dependence on t_{FeMn}, presenting a high value for approximately the first 3 ML $Fe_{50}Mn_{50}$, decreasing upon increasing $Fe_{50}Mn_{50}$ thickness, and reaching an apparently constant value for $t_{FeMn}>6$ ML. For comparison the asymmetry of the Co image in the same sample area, extracted from the rectangle printed in Fig. 4(a), is displayed by the dash-dotted line in Fig. 6. One can see that the asymmetry of Co is almost constant along the $Fe_{50}Mn_{50}$ slope. The thickness dependence of the Fe asymmetry in an $Fe_{50}Mn_{50}$ wedge suggests that in the first stage of growth on a magnetic Co film, all the Fe moments are ferromagnetically aligned. Indeed the value of asymmetry measured in this region ($\approx 16\%$) is similar to the value measured on a thick Fe film grown on $W(001)$ (15.7%), which can be considered as a standard value of bulk Fe for the present experimental geometry and degree of polarization.[22] The decreasing of the Fe asymmetry by increasing the FeMn thickness is consistent with the hypothesis that the observed net magnetic moment of Fe is located at the interface with Co. It is important to check the behavior of the induced net moment in Fe for the reversed order of deposition, that is when a ferromagnetic Co film is deposited on top of $Fe_{50}Mn_{50}$. The Fe asymmetry as a function of t_{FeMn} for this case is displayed in Fig. 6 by the dotted line (again the sketch of the sample is given). The general trend is very similar to the case of $Fe_{50}Mn_{50}$ deposited on Co (solid line). Therefore, the hypothesis of an induced net moment at the interface is plausible also in this case. Actually this model would lead to a different value of the asymmetry

for high FeMn thickness, while the solid and the dotted curves exhibit an almost identical value for $t_{FeMn} > 6$ ML. Further experiments are needed to understand this discrepancy and to build up a correct picture of the dependence of the induced net moment as a function of the $Fe_{50}Mn_{50}$ thickness, especially in the first stages of growth.

To illustrate the size of the observed moment in Fe, we will analyze the following model: We assume that the induced net moment is caused by Fe atoms in the interface layer only, which are fully aligned with the Co moments, while all other Fe atoms have either no moment or perfectly compensate each other. In a continuous thickness model, t_M shall denote the thickness of the interface region of the FeMn layer which gives rise to the observed asymmetry. Fe atoms from this interface region contribute a fraction R to the measured Fe absorption signal. For the Co/FeMn/Cu(001) system R can be expressed as

$$R = \frac{\int_0^{t_M} \exp^{-x/\lambda} dx}{\int_0^{t_{FeMn}} \exp^{-x/\lambda} dx}, \tag{1}$$

where λ is the effective escape depth of the secondary electrons. Equation (1) can be solved for t_M as

$$t_M = -\lambda \ln[1 - R(1 - \exp^{-t_{FeMn}/\lambda})]. \tag{2}$$

If the Fe atoms from the interface region exhibit a dichroic asymmetry of A_0, the measured asymmetry will be RA_0 if the rest of the film does not contribute a magnetic asymmetry. The value of maximum contrast between two oppositely magnetized domains measured in the Fe images in $Fe_{50}Mn_{50}$ is 1.3% for $t_{FeMn} = 12$ ML, while $A_0 = 15.7\% \times 2 = 31.4\%$ for a thick Fe standard. Considering this ratio R of 0.04, assuming further a probing depth of 20 Å,[10] in which the secondary electron signal is reduced by a factor of $1/e$, and taking the lattice spacing of $Fe_{50}Mn_{50}$ layers as 1.81 Å,[24] one obtains from Eq. (2) $t_M = 0.3$ ML.[23] This estimate would mean that the observed asymmetry could be caused by about 30% of the Fe atoms in the interfacial ML that have their bulk moment fully aligned with the Co magnetization. Considering that an $Fe_{50}Mn_{50}$ film grows epitaxially on Cu(001),[14] the area density of the Fe atoms is 7.65×10^{14} atoms/cm^2 and one may calculate the atom area density of the fully aligned Fe atoms as 2.30×10^{14} atoms/cm^2. A similar estimation is not possible for Mn, since no value of the asymmetry for FM bulk Mn is available. In general, the measured Mn asymmetry in different samples is not as constant as for Fe. Moreover, whereas the domains of the induced Fe moments are always found with the magnetization in the same direction as the Co ones, Mn is sometimes coupled antiparallel to Co and Fe. These particular features of the induced net moment in Mn will be discussed in more detail below.

As mentioned above, below about 3-ML FeMn thickness, the Fe asymmetry exhibits the same value as expected for a fully ferromagnetic Fe film, $R = 1$ in the above model, or $t_M = t_{FeMn}$. In this case the presence of the FM Co layer induces the full ferromagnetic alignment of all Fe atoms in the $Fe_{50}Mn_{50}$ film. The amount of aligned Fe moments decreases then for increasing FeMn thickness, until at above ≈ 7 ML it corresponds to the above calculated $t_M = 0.3$ ML. This means that upon increasing the FeMn thickness, most of the initially aligned Fe moments of a 3 ML $Fe_{50}Mn_{50}$ film on Co go back to a paramagnetic or antiferromagnetic state. This is likely due to the increasing antiferromagnetic interactions in the FeMn film compared to the FM interaction with the Co layer when the thickness gets larger.

An induced moment in a non-FM material by proximity of an FM material is actually a general observation in thin-film magnetism, dating back to the magnetization of Pd films by interaction with FM Ni films.[25] Indeed small net magnetic moments, induced by proximity of FM materials, have been found in antiferromagnets like Cr[19] and also in nonmagnetic metallic materials like V,[26] Pt,[27] and Cu in contact with Co (Ref. 28) or with Fe.[29] Hybridization effects of the *d* electrons are generally claimed to give rise to such observations.

The partial uncompensation of moments in an antiferromagnet in contact with a ferromagnet could be important in order to understand the exchange bias phenomenon. The present experiments have provided evidence that the contact with the Co film induces a net magnetic moment in Fe and Mn, no matter whether $Fe_{50}Mn_{50}$ is in a PM state (for $t_{FeMn} < 10$ ML) or in an AFM state (for $t_{FeMn} > 10$ ML). In particular, when the alloy is in an AFM state one could be tempted to consider the measured induced net moment as AFM *uncompensated* moments leading to exchange bias. This is actually not completely true. AFM uncompensated moments are, by definition, moments of atoms in an AFM atomic plane which sum up to give a nonvanishing net magnetization in that plane. Because of the depth-dependent weighting of the XMCD signal in PEEM, such uncompensated moments could be indeed observed as a net magnetic moment. The net moments in Fe and Mn reported here, however, have been measured also when the $Fe_{50}Mn_{50}$ film is PM, where they fully participate to the FM phase of Co. When $Fe_{50}Mn_{50}$ is AFM, *a small part* of the measured asymmetry could indeed be given by AFM uncompensated moments. While most of the observed net moments have their magnetization direction always aligned with the Co magnetization direction, thus still participating to the FM phase of Co, a small fraction of uncompensated moments should be pinned to the direction imposed by the AFM spins in order to give rise to the shift in the hysteresis loop. These uncompensated moments are then only in the direction of the Co magnetization when the $Fe_{50}Mn_{50}$ film is deposited on top of Co, or after a field or remanent cooling procedure. Once this direction is established they will not rotate upon switching the Co magnetization, thus leading to the exchange bias effect.

From an intuitive point of view, the origin of the observed Fe and Mn XMCD asymmetry in the AFM $Fe_{50}Mn_{50}$ alloy can be explained by considering the noncollinear AFM spin structure of $Fe_{50}Mn_{50}$ as taken from the bulk.[20] According to this spin structure, an ideal (001) terminated surface exhibits in-plane projections of the spins directed along two opposite $\langle 110 \rangle$ directions, for example $\pm[110]$. The neighboring

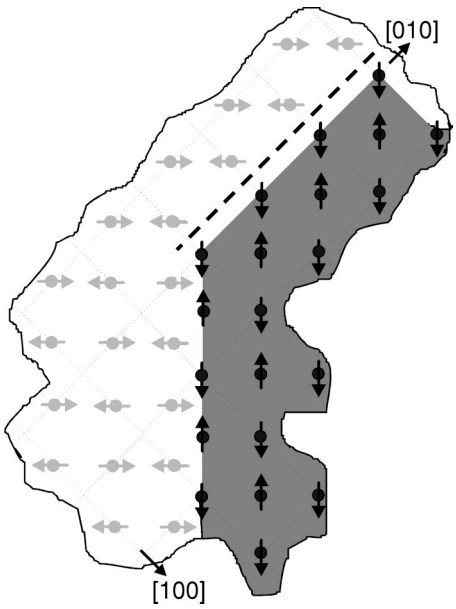

FIG. 7. Schematic representation of the top view of a topological domain, created by a 1 ML step, at the (001) surface of $Fe_{50}Mn_{50}$ with the bulk spin structure. The spins adjacent to the dashed line are uncompensated. The in-plane crystallographic axes are indicated.

atomic planes, above or below, then exhibit spins with their in-plane component rotated by 90°, i.e., directed along $\pm[\bar{1}10]$. A small twist of these AFM axes towards the magnetization direction of the adjacent Co film would give rise to a small uncompensated magnetic moment in the interface plane of the $Fe_{50}Mn_{50}$ film, which may or may not be compensated by a corresponding twist in the deeper layers. Such a twist would not lead to exchange bias, since the induced net moment would always switch together with the FM layer. Actually the presence of a net magnetic moment in the AFM FeMn film, being consistent with this model, could arise also in case of other spin structures. For example, a net magnetic moment would be observed by XMCD-PEEM if the FeMn alloy was characterized by a collinear layerwise AFM order, as concluded from the calculations of Ref. 30, or even for a more complicated spin structure.

Uncompensated moments that are leading to exchange bias could be located at topological AFM domain boundaries, created by monoatomic steps at the AFM ordered $Fe_{50}Mn_{50}$ surface. An example is given in Fig. 7. The top view of a portion of the $Fe_{50}Mn_{50}$ surface, where a topological domain created by a 1 ML high step is present, is schematically displayed. The surface of the gray domain is, for example, 1 ML above the white domain. The in-plane crystallographic axes are indicated. The direction of the AFM spins, represented by the arrows, is along the $\langle 110\rangle$ in-plane directions. If the step runs along one of the $\langle 100\rangle$ axes, the spins at the step edge are uncompensated, as one can see by considering the spins adjacent to the black dashed line, where they sum up to give a net component along $[0\bar{1}0]$.

The fraction of interface atoms sitting at step edges in the $Fe_{50}Mn_{50}$ film may be estimated from Fig. 1. A number of about 2% of the interface atoms being at step edges is obtained from that figure, most of which are running along $\langle 110\rangle$ directions. Such uncompensated step edge atoms would thus indeed constitute only a minor contribution to the observed asymmetry in the Fe and Mn images.

The effective influence of the uncompensated $Fe_{50}Mn_{50}$ moments on the coupling at the interface with Co is actually difficult to quantify from the asymmetry images of Fe and Mn. This is related to the fact that the signal from the induced net magnetic moment is already quite low, and that, as mentioned above, the uncompensated moments are probably just a small fraction of this moment. One can see this by considering that the observed asymmetry does not change appreciably when $Fe_{50}Mn_{50}$ is PM or AFM, and that uncompensated moments should not be present when the alloy film is paramagnetic. Moreover, the uncompensated moments should mediate the coupling between the FM and the AFM layer in the way explained above. In Ref. 21 an oscillation in the coupling strength in Co/FeMn bilayers on Cu(001) has been deduced from a 1 ML oscillation in the coercivity. If this interpretation was correct, also the value of the uncompensated moments responsible for the coupling should oscillate with a period of 1 ML. In the Fe and Mn images, however, such a behavior of the asymmetry is not present, as one sees in the Fe case from Fig. 4(d) for $t_{FeMn} > 10$ ML. This can be explained by considering that most part of the obtained asymmetry is not given by these uncompensated moments, the oscillating behavior of which as a function of the $Fe_{50}Mn_{50}$ thickness is therefore hidden below the noise level ($\approx 2\%$ of the induced moments).

The induced net moment in Mn deserves some more comments. While the asymmetry in Fe (and therefore the value of the induced net moment) has always been found similar in all the samples imaged with the PEEM, a different behavior has been observed for Mn. In fact the asymmetry value, being usually slightly smaller than that measured in Fe, in some samples has been found higher than the Fe one, in some others so small that domain images could not be detected. Moreover, while the induced moment in Fe was always found parallel to the Co film magnetization, the domains in Mn have been found in some cases magnetized in the same direction as the Co and Fe ones (see Fig. 2), in some other cases in the opposite direction, as in Fig. 3. These somehow puzzling observations about the induced moments in Mn can be explained considering that the magnetic state of the Mn atoms is very sensitive to oxidation and to the magnetic environment in which they are located. For example, contradictory reports have been published about the orientation of the magnetization in submonolayer Mn films on top of FM Fe substrates, either parallel or antiparallel with respect to the substrate magnetization.[31,32] The Mn magnetization reduces to zero or changes from parallel to antiparallel with respect to the underlying Fe by oxygen adsorption.[33] Another mechanism which can influence the amount and the direction of the induced moment in Mn in the $Fe_{50}Mn_{50}$ films is the local interaction of Mn atoms with the Fe and Co atoms. In dilute FM CoMn and FeMn alloys, the Mn magnetization has been found by XMCD to be aligned parallel to Co in a $Co_{94}Mn_6$ thin-film alloy,[34] while magnetic reflectivity experiments revealed antiparallel orientation of Fe and Mn magne-

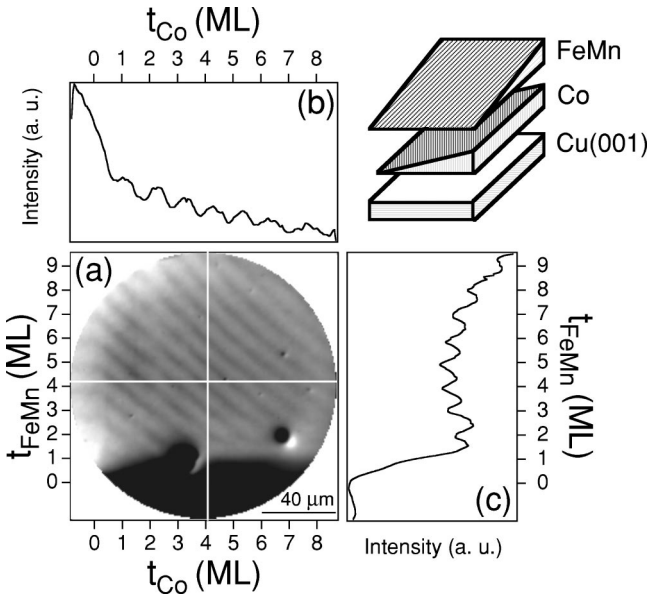

FIG. 8. (a) PEEM image obtained by excitation with a Hg discharge lamp of an $Fe_{50}Mn_{50}$/Co double-wedge bilayer on Cu(001). A sketch of the sample is given in the upper right corner of the figure. Co and $Fe_{50}Mn_{50}$ thicknesses are indicated at the image axes. Panels (b) and (c) display linescans of the intensity measured along the horizontal and vertical white lines in image (a), respectively.

tization in an $Fe_{90}Mn_{10}$ alloy.[35] This would suggest that preferentially the Mn atoms tend to couple antiferromagnetically to Fe and ferromagnetically to Co, at least when alloying. From these considerations one may therefore expect that local differences in composition or in amount of roughness in nominally identical films may induce a locally different environment for the Mn atoms. For example, the number of Fe or Co atoms surrounding the Mn atoms may vary. Considering the different interactions that come into play, that is Mn-Mn, Mn-Fe, and Mn-Co, one could therefore expect that also the amount and the direction of the induced net magnetic moments may change.

Finally, an interesting effect present in some of the Mn images is the superposition of regular stripes of alternating contrast on the domain pattern. These are shown in the Mn image of Fig. 5. From this figure one sees that the stripes are perpendicular to the gradient of total thickness. Indeed the period of the stripes in the vertical and horizontal directions corresponds to 1 ML in the $Fe_{50}Mn_{50}$ and Co thicknesses, respectively. Stripes having 1 ML period may not have a magnetic origin, but they can be merely caused by a periodic change in the topology of the wedged film. Indeed during the layer-by-layer growth of the Co/$Fe_{50}Mn_{50}$ bilayers on Cu(001), the number of surface steps oscillates with monolayer period, as indicated by the presence of 1 ML period oscillations in the medium energy electron diffraction intensity during the deposition of the bilayer.[14] In order to verify this hypothesis, an $Fe_{50}Mn_{50}$/Co double-wedge sample, in which stripes in the Mn images were present, was illuminated by a Hg discharge lamp. The resultant image is shown in Fig. 8(a). The $Fe_{50}Mn_{50}$ and Co thicknesses of the imaged area are indicated at the left axis, increasing from bottom to top, and at the bottom axis, increasing from left to right, respectively. In the figure a schematic sketch of the sample is given. Since the photon energy of the Hg lamp is around 4.9 eV, the emitted electrons are those with a final energy just slightly above the work-function threshold of the material. The contrast of Fig. 8(a) arises therefore from local differences in the work function due to structural and topological features of the sample surface, and it does not contain magnetic information.[36] Still stripes of alternating gray scale contrast are present, which are the same as those observed in some of the Mn L_3 images. Obviously now the stripes are not superimposed on magnetic domains, and the intensity difference of adjacent stripes is higher than in the Mn L_3 images. One can perform a scan along the horizontal and the vertical directions in the image, in order to check the stripes' period, and compare it to the film thickness. These line scans have been performed along the horizontal and vertical white lines printed in Fig. 8(a), and are reported in Fig. 8(b) and Fig. 8(c), respectively. In Fig. 8(b) the intensity (left axis) is plotted as a function of the Co thickness at the upper axis. In Fig. 8(c) the intensity is at the bottom axis, and the $Fe_{50}Mn_{50}$ thickness at the right axis. One can see that the oscillations in the intensity, corresponding to different gray scale contrast in the stripes, have a period of 1 ML in both the Co and the $Fe_{50}Mn_{50}$ thickness. Actually one cannot identify without uncertainty whether a maximum or a minimum in the intensity oscillations corresponds to the completion of an integer number of monolayers. In fact while the 10% error in the thickness calibration is only 0.1 ML in the determination of the period of the oscillations, it amounts to almost 1 ML in the absolute thickness at 9 ML, therefore impeding definitive conclusions about the phase of the oscillations. Since the contrast in Fig. 8 is of topological origin, a possible explanation of stripes of different intensity having a period of 1 ML is the periodic variation of the number of surface steps, considering roughness induced work-function changes.[37] The fact that these stripes were observed also in the Mn domain images, and not in the Fe and Co images, can be explained by considering that the topological origin of the stripes induces an intensity difference between adjacent stripes. In this case a slight difference in intensity between the right and left polarized light can give rise to a nonvanishing term when one calculates the asymmetry. Moreover, Mn, among the three materials considered here, is the one with the lowest binding energy. Therefore the edge intensity of Mn from a Co/$Fe_{50}Mn_{50}$ sample has the lowest background, thus enhancing this effect.

V. CONCLUSION

By using PEEM and XMCD as magnetic contrast mechanism, magnetic domain images have been obtained from Co, Fe, and Mn in interacting Co-FeMn single-crystal bilayers on Cu(001). A net magnetic moment is induced in Fe and Mn when the Co film is in contact with $Fe_{50}Mn_{50}$, both in the PM and the AFM state of $Fe_{50}Mn_{50}$. In the case of Fe, this induced moment, if confined to the interface with Co, would amount to approximately 30% of the interfacial Fe atoms being fully aligned with the Co magnetization while having

the Fe bulk magnetic moment. Mn domain images could be detected in which the direction of the net magnetic moment was either parallel or antiparallel to Co and Fe. This is related to the sensitivity of the magnetic state of the Mn atoms to the structural and magnetic environment in which they are embedded. Part of the induced net moment measured in Fe and Mn could consist of uncompensated AFM spins. However, due to the rather low magnetic signal, it is quite difficult to distinguish the part strongly coupled to the AFM lattice spins, giving rise to the exchange bias effect, and the part rotating upon switching the magnetization of the Co layer.

ACKNOWLEDGMENTS

We would like to thank B. Zada for her expert technical support, and the staff of the Bessy II Berlin synchrotron radiation facility and W. Mahler for valuable help during the beamtime. Financial support by the German Minister for Education and Research (BMBF) under Grant No. 05 KS1EFA 6 is gratefully acknowledged.

*Present address: INFM, Unità Roma Tre, Via della Vasca Navale 84, I-00146 Roma, Italy.

†Corresponding author. Electronic address: kuch@mpi-halle. de

[1] J. Nogués and I.K. Schuller, J. Magn. Magn. Mater. **192**, 203 (1999).

[2] M. Kiwi, J. Magn. Magn. Mater. **234**, 584 (2001).

[3] J.C.S. Kools, IEEE Trans. Magn. **32**, 3165 (1996).

[4] W.H. Meiklejohn and C.P. Bean, Phys. Rev. **105**, 904 (1957).

[5] T.C. Schulthess and W.H. Butler, J. Appl. Phys. **85**, 5510 (1999).

[6] K. Takano, R.H. Kodama, A.E. Berkowitz, W. Cao, and G. Thomas, Phys. Rev. Lett. **79**, 1130 (1997).

[7] W.J. Antel, Jr., F. Perjeru, and G.R. Harp, Phys. Rev. Lett. **83**, 1439 (1999).

[8] C. Sánchez-Hanke and C.-C. Kao, J. Magn. Magn. Mater. **226-230**, 1803 (2001).

[9] H. Ohldag, T.J. Regan, J. Stöhr, A. Scholl, F. Nolting, J. Lüning, C. Stamm, S. Anders, and R.L. White, Phys. Rev. Lett. **87**, 247201 (2001).

[10] R. Nakajima, J. Stöhr, and Y.U. Idzerda, Phys. Rev. B **59**, 6421 (1999).

[11] F. Nolting, A. Scholl, J. Stöhr, J.W. Seo, J. Fompeyrine, H. Siegwart, J.P. Locquet, J. Lüning, E.E. Fullerton, M.F. Toney, M.R. Scheinfein, and H.A. Padmore, Nature (London) **405**, 767 (2000).

[12] J. Stöhr, A. Scholl, T.J. Regan, S. Anders, J. Lüning, M.R. Scheinfein, H.A. Padmore, and R.L. White, Phys. Rev. Lett. **83**, 1862 (1999).

[13] H. Ohldag, A. Scholl, F. Nolting, S. Anders, F.U. Hillebrecht, and J. Stöhr, Phys. Rev. Lett. **86**, 2878 (2001).

[14] F. Offi, W. Kuch, and J. Kirschner, Phys. Rev. B **66**, 064419 (2002).

[15] W. Kuch, J. Gilles, F. Offi, S.S. Kang, S. Imada, S. Suga, and J. Kirschner, J. Electron Spectrosc. Relat. Phenom. **109**, 249 (2000).

[16] J. Stöhr, H.A. Padmore, S. Anders, T. Stammler, and M.R. Scheinfein, Surf. Rev. Lett. **5**, 1297 (1998).

[17] W. Swiech, G.H. Fecher, Ch. Ziethen, O. Schmidt, G. Schönhense, K. Grzelakowski, C.M. Schneider, R. Frömter, H.P. Oepen, and J. Kirschner, J. Electron Spectrosc. Relat. Phenom. **84**, 171 (1997).

[18] C.M. Schneider, J. Magn. Magn. Mater. **175**, 160 (1997).

[19] W. Kuch, R. Frömter, J. Gilles, D. Hartmann, C. Ziethen, C.M. Schneider, G. Schönhense, W. Swiech, and J. Kirschner, Surf. Rev. Lett. **5**, 1241 (1998).

[20] H. Umebayashi and Y. Ishikawa, J. Phys. Soc. Jpn. **21**, 1281 (1966).

[21] W. Kuch, F. Offi, L.I. Chelaru, M. Kotsugi, K. Fukumoto, and J. Kirschner, Phys. Rev. B **65**, 140408 (2002).

[22] The Fe/W(001) sample was imaged with similar PEEM and beamline settings as the $Co/Fe_{50}Mn_{50}$ bilayers.

[23] From Eq. (2) one may calculate that a variation of λ from 10 Å to 100 Å leads to a variation of t_M from 0.2 ML to 0.4 ML, respectively.

[24] Y. Endoh and Y. Ishikawa, J. Phys. Soc. Jpn. **30**, 1614 (1971).

[25] U. Gradmann and R. Bergholz, Phys. Rev. Lett. **52**, 771 (1984).

[26] A. Scherz, H. Wende, P. Poulopoulos, J. Lindner, K. Baberschke, P. Blomquist, R. Wäppling, F. Wilhelm, and N.B. Brookes, Phys. Rev. B **64**, 180407 (2001).

[27] S. Ferrer, J. Alvarez, X. Torrelles, E. Lundgren, and P. Fajardo, Physica B **248**, 9 (1998).

[28] M.G. Samant, J. Stöhr, S.S.P. Parkin, G.A. Held, B.D. Hermsmeier, F. Herman, M. van Schilfgaarde, L.-C. Duda, D.C. Mancini, N. Wassdahl, and R. Nakajima, Phys. Rev. Lett. **72**, 1112 (1994).

[29] W. Kuch, M. Salvietti, X. Gao, M.-T. Lin, M. Klaua, J. Barthel, Ch.V. Mohan, and J. Kirschner, Phys. Rev. B **58**, 8556 (1998).

[30] D. Spišák and J. Hafner, Phys. Rev. B **61**, 11 569 (2000).

[31] see, for example, S. Andrieu, M. Finazzi, Ph. Bauer, H. Fischer, P. Lefevre, A. Traverse, K. Hricovini, G. Krill, and M. Piecuch, Phys. Rev. B **57**, 1985 (1998), and references therein.

[32] see, for example, T. Igel, R. Pfandzelter, and H. Winter, Phys. Rev. B **58**, 2430 (1998), and references therein.

[33] O. Rader, C. Pampuch, W. Gudat, A. Dallmeyer, C. Carbone, and W. Eberhardt, Europhys. Lett. **46**, 231 (1999).

[34] S. Banerjee, W.L. O'Brien, and B.P. Tonner, J. Magn. Magn. Mater. **198-199**, 267 (1999).

[35] A. Déchelette, J.M. Tonnerre, M.C. Saint Lager, F. Bartolomé, L. Sève, D. Raoux, H. Fischer, M. Piecuch, V. Chakarian, and C.C. Kao, Phys. Rev. B **60**, 6636 (1999).

[36] Magnetic contrast by using a PEEM in threshold photoemission has been actually demonstrated by G.K.L. Marx, H.J. Elmers, and G. Schönhense, Phys. Rev. Lett. **84**, 5888 (2000), for FM materials; and N.B. Weber, C. Bethke, and F.U. Hillebrecht, J. Magn. Magn. Mater. **226-230**, 1573 (2001), for AFM materials. In both cases, however, magnetic contrast was obtained from the asymmetry of two images and it was lower than the corresponding magnetic contrast after excitation at the core level edges.

[37] D.P. Woodruff and T.A. Delchar, *Modern Techniques of Surface Science*, 2nd ed. (Cambridge University Press, Cambridge, 1994), p. 461 and following.